ELSEVIER

Application of a near-wall turbulence model to the flows over a step with inclined wall

Jong Woo Ahn
Korea Research Institute of Ships and Ocean Engineering, KIMM, Daeduck Science Town, Taejon, Korea,

Tae Seon Park and Hyung Jin Sung
Korea Advanced Institute of Science and Technology, Kusong-dong, Yusong-gu, Taejon, Korea

A nonlinear low-Reynolds-number k-ε model of Park and Sung (1995) was extended to predict the flows over a step with inclined wall, where a boundary-layer flow without separation and a separated and reattaching flow coexist. For a better prediction of the flows, a slight modification was made on the function of wall damping f_μ and the model constant $C_{\varepsilon 1}$ in the ε-equation. The model performance was validated by comparing the model predictions with the experiment. It was shown that the flows over a step with inclined wall are simulated successfully with the present model. © 1997 by Elsevier Science Inc.

Introduction

Turbulent flow over a backward-facing step is frequently employed for benchmarking the performance of turbulence models for separated and reattaching flows. If a turbulence model can reproduce this flow correctly, then the possibilities that the model is equally successful with other types of turbulent flows would be high. Separated and reattaching flows are encountered in a host of practical engineering situations. The flow separation and subsequent reattachment processes generate extremely complex flow characteristics. Among others, the separated flow, which then reattaches in the downstream locations, gives rise to flow unsteadiness, pressure fluctuations, noise, etc. Also, flow separation tends to enhance mixing. It is, therefore, desirable to develope a new turbulence model for separated and reattaching flows, and an accurate prediction poses a significant and challenging task (Abe et al. 1994; Avva et al. 1988; So et al. 1988).

A literature survey reveals that considerable attention has been given to the development of turbulence models, which can resolve separated and reattaching flows satisfactorily. Among the various turbulence models, the k-ε turbulence model is widely used owing to its simplicity and effectiveness rather than more sophisticated higher-order model (Nagano and Tagawa 1990; Patel et al. 1985; Yap 1987). Recently, an improved version of the nonlinear low Reynolds number k-ε model has been developed by Park and Sung (1995). In their model, the limiting near-wall behavior and nonlinear Reynolds stress representations were incorporated. The main emphasis was placed on the adoption of $R_y(\equiv k^{1/2}y/\nu)$ instead of $y^+(\equiv u_\tau y/\nu)$ in the low-Reynolds-number model to avoid the difficulties at the separation and reattaching points ($u_\tau = 0$). The nonequiliblium effect was also taken into account to describe recirculating flows away from the wall. Their model was validated by applying to an attached boundary layer flow and by solving the benchmark problem of turbulent flow behind a backward-facing step. The model performance was shown to be generally satisfactory.

In the present study, the preceding Park and Sung (1995) model (hereafter referred to as PS model) is applied to stimulate the flows over a step with inclined wall. As sketched in Figure 1, by varying the wall inclination angle α, two typical flow configurations coexist. For a small α, a boundary-layer flow is present without separation; whereas, a separated and reattaching flow takes place for a large value of α. This flow configuration is a good example to test the turbulence model performance. A laboratory measurement has been made by Ruck and Makiola (1993), in which the aim was to determine the differences in turbulent flow field quantities compared to the 90° step geometry. The inclination angle was varied between 10 and 90° at high Reynolds number $Re_H = 30{,}800$. As Ruck and Makiola remarked of their experiment, the main contributions were to understand the phenomena of separated flows and to establish a comprehensive database for the validation of numerical simulations.

As an extention of the model performance, the model of Park and Sung (1995) has been applied to the flows over a step with inclined wall. By varying the wall inclination angle, the predicted results were compared with the experimental data of Ruck and Makiola (1993). An extensive model test indicates that a slight modification of the PS model is needed. The main reason for a modification may be because the PS model has been developed on the basis of two extreme cases; i.e., the boundary-layer flow ($\alpha = 0°$) and the flow over a backward-facing step ($\alpha = 90°$). Actually, as we applied the PS model to the flows over a step with inclined wall, the predicted reattachment lengths were found to be slightly overpredicted except the case $\alpha = 90°$; i.e., the flow over a backward-facing step. The main objective of the present study is to extend the PS model, which can give a better prediction result to the flows over a step with inclined wall. Based on the PS model, the modification is made on the function of f_μ and the model constant $C_{\varepsilon 1}^*$. Details regarding the model imple-

Address reprint requests to Professor H. J. Sung, Dept. of Mechanical Engineering, Korea Advanced Institute of Science & Technology, 373-1 Kusong-dong, Yusong-gu, Taejon, 305-701, South Korea.
Received 17 February 1996; accepted 9 August 1996

Int. J. Heat and Fluid Flow 18:209-217, 1997

655 Avenue of the Americas, New York, NY 10010

0142-727X/97/$17.00
PII S0142-727X(96)00092-9

mentations are recapitulated in the following sections. The predicted results are compared against the output of the model of Abe et al. (1994) (hereafter referred to as the AKN model) as well as the experimental data. It is shown that the flows over a step with inclined wall are simulated successfully with the present model.

Low-Reynolds-number k-ε model

Governing equations

For a stationary, incompressible turbulent flow, the governing equations can be written in Cartesian tensor notations as

$$\frac{\partial U_i}{\partial x_i} = 0 \tag{1}$$

$$U_j \frac{\partial U_i}{\partial x_j} = -\frac{1}{\rho}\frac{\partial P}{\partial x_i} + \frac{\partial}{\partial x_j}\left(\upsilon \frac{\partial U_i}{\partial x_j} - \overline{u_i u_j}\right) \tag{2}$$

where U_j and u_j are the jth components of the mean and fluctuating velocities, respectively. P is the mean pressure, ρ and υ are the fluid density and kinematic viscosity, respectively. The unknown Reynolds stress $-\overline{u_i u_j}$ can be expressed, by using the concept of eddy-viscosity υ_t:

$$\begin{aligned} -\overline{u_i u_j} = {} & 2\upsilon_t S_{ij} - \frac{2}{3}k\delta_{ij} \\ & + C_{s1}\upsilon_t \frac{k}{\varepsilon}\left(S_{im}S_{mj} - \frac{1}{3}S_{mn}S_{mn}\delta_{ij}\right) \\ & + C_{s2}\upsilon_t \frac{k}{\varepsilon}(\omega_{im}S_{mj} \\ & + \omega_{jm}S_{mi}) + C_{s3}\upsilon_t \frac{k}{\varepsilon}\left(\omega_{im}\omega_{jm} - \frac{1}{3}\omega_{mn}\omega_{mn}\delta_{ij}\right) \end{aligned} \tag{3}$$

$$\upsilon_t = C_\mu f_\mu \frac{k^2}{\varepsilon} \tag{4}$$

$$U_j \frac{\partial k}{\partial x_j} = \frac{\partial}{\partial x_i}\left[\left(\upsilon + f_t \frac{\upsilon_t}{\sigma_k}\right)\frac{\partial k}{\partial x_j}\right] + P_k - \varepsilon \tag{5}$$

$$U_j \frac{\partial \varepsilon}{\partial x_j} = \frac{\partial}{\partial x_j}\left[\left(\upsilon + f_t \frac{\upsilon_t}{\sigma_\varepsilon}\right)\frac{\partial \varepsilon}{\partial x_j}\right] + P_\varepsilon^1 + P_\varepsilon^2 + P_\varepsilon^3 + P_\varepsilon^4 - \Gamma \tag{6}$$

In the above equations, $-\overline{u_i u_j}$ is expanded up to the second-order term in a nonlinear k-ε model, where S_{ij} and ω_{ij} represent the mean strain rate tensor and mean vorticity tensor, respectively. C_{s1}, C_{s2}, C_{s3}, and C_μ are the model constants: $C_{s1} = 0.6$, $C_{s2} = 0.4$, $C_{s3} = 0.005$, $C_\mu = 0.09$. It is noted that the fourth term in Equation 3, pure rotation term, has been deleted in the present study ($C_{s3} = 0$). This is based on the fact that the pure rotation term can create the anisotropy by pure rotation for initially isotropic turbulence. This is incorrect behavior according to both the direct numerical simulation (DNS) and the rapid distortion theory (Lee et al. 1990). The f_μ function reflects the effects of wall proximity and low-Reynolds-number. The production of turbulent energy P_k is defined as $P_k \equiv -\overline{u_i u_j}\partial U_i/\partial x_j$. f_t represents the model function for turbulent diffusion. The model constant σ_k and σ_ϵ in the turbulent diffusion terms of k and ε are taken to be $\sigma_k = 1.2$ and $\sigma_\varepsilon = 1.3$ with a modified model function $f_t = 1 + 2.0\,exp[-(R_t/150)^2]$ (Nagano and Shimada 1993). Here, R_t represents the turbulent Reynolds number $R_t = k^2/\upsilon\varepsilon$. In the ε-equation, P_ε^1, P_ε^2, P_ε^3, P_ε^4, and Γ represent the mixed production, production by mean velocity gradient, gradient production, turbulent production, and destruction in sequence, respectively.

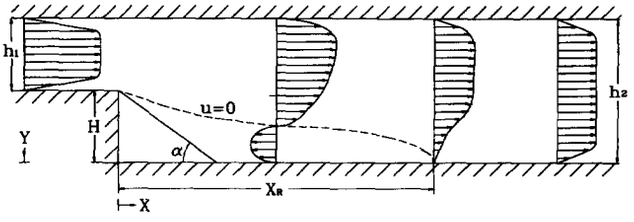

Figure 1 Schematic configuration of the flow over a step with inclined walls

Model function of f_μ

In many previous models for representing the wall-proximity effects, the form similar to the Van Driest damping function has been used, in which the model constant C_μ is set to be constant ($C_\mu = 0.09$). When f_μ is introduced to predict the damping of eddy-viscosity near the wall, then f_μ must approach 1 far from the wall, which indicates that the standard k-ε model form is recovered. However, the local equilibrium ($P_k = \varepsilon$) is no longer satisfied in the recirculating region away from the wall. To incorporate the nonequilibrium effect ($P_k \neq \varepsilon$), variations of C_μ are allowed in the present study; i.e., $f_\mu = f_{\mu 1} f_{\mu 2}$. By using this expression, it is intended that f_μ takes into account the two major dynamic effects; $f_{\mu 1}$ signifies the effect of wall proximity in the near-wall region, and $f_{\mu 2}$ represents the effect of nonequilibrium away from the wall.

In the first, the effect of wall-proximity in the near-wall region is inspected. The $f_{\mu 1}$ function is generally employed as the similar form of the PS model (1995).

$$f_{\mu 1} = (1 - f_{w1})(1 + 200 f_{w1}/R_t^{1.25}) \tag{7}$$

$$f_{w1} = \exp\left[-(R_y/70)^2\right] \tag{8}$$

The wall-reflection function f_{w1} represents the effect of wall-proximity. A closer inspection of Equations 7 and 8 discloses that new model constants were adopted as compared with the original PS model. The new values were proven to give a more accurate prediction with the DNS data (Mansour et al. 1988). Needless to say $f_{\mu 1}$ satisfies the limiting behavior $f_{\mu 1} \propto y^{-1}$.

Next, the effect of nonequilibrium away from the wall is demonstrated ($f_{\mu 2}$). It has been known that C_μ varies as a function of P_k/ε, away from the wall ($f_{\mu 1} = 1$), as addressed in the experimental findings of Rodi (1972). To formulate the C_μ form in the nonequilibrium region away from the wall, the model of Launder (1982) is employed, among others, in the present study. This is because the predictability of their models is found to be satisfactory in the light of accuracy and convergency. Launder formulated the Reynolds stress $-\overline{u_i u_j}$ by introducing a set of algebraic stress models. However, it was found that, as the scale of eddy becomes larger, its contribution to convective and diffusive transports is dominant. To alleviate this factor, the convection and diffusion terms were approximated; i.e., a preferential transport of off-diagonal Reynolds stresses was allowed. The detailed derivations can be found in Launder. The f_{u2} form, in which the nonequilibrium parameter P_k/ε is included, is

obtained by rearranging the formula with some modifications,

$$f_{\mu 2} = 2.75 \frac{[0.9 + 0.85(P_k/\varepsilon) + 1.1(D_k/\varepsilon)]}{[0.9 + 1.3(P_k/\varepsilon) + 1.1(D_k/\varepsilon)]} \tag{9}$$

In the above, D_k/ε represents the ratios of diffusive gain of turbulence energy to viscous loss

$$D_k = 2\upsilon \left(\frac{\partial \sqrt{k}}{\partial x_j} \right)^2 .$$

Modeling of the ε-equation

By following the scaling argument of Rodi and Mansour (1993) the P_ε^1, P_ε^2, P_ε^3, P_ε^4, and Γ terms in Equation 6 can be modeled in a way similar to the prior models,

$$P_\varepsilon^1 + P_\varepsilon^2 + P_\varepsilon^4 - \Gamma = C_{\varepsilon 1}^* P_k \frac{\varepsilon}{k} - C_{\varepsilon 2} f_2 \frac{\varepsilon^2}{k} \tag{10}$$

where $C_{\varepsilon 1}^*$ and $C_{\varepsilon 2}$ are the model constants. It is revealed that the model constant $C_{\varepsilon 1}^*$ is sensitive to the nonequilibrium effect (P_k/ε) (Park and Sung 1995; Durbin 1993). In other words, $C_{\varepsilon 1}^*$ gives a significant influence on the reattachment length (X_R) in a separated and reattaching flow. As emphasized in the introduction, if we applied the PS model for the flow over a step with inclined walls, slight overpredictions of the reattachment length were detected. To improve the result, a modified model constant is proposed in the present study; i.e., $C_{\varepsilon 1}^* = C_{\varepsilon 1}(0.98 + 0.02P_k/\varepsilon)$. By utilizing the present model constant, the additional production of dissipation by local anisotropy (P_k/ε) is properly taken into consideration. However, the model constants $C_{\varepsilon 1}$ and $C_{\varepsilon 2}$ are set to take the standard values of 1.45 and 1.9, respectively.

The model function f_2, which deals with the sum of source and sink terms in the near-wall region, is defined as

$$f_2 = (1 + f_{21})(1 - f_{w2}) f_{22} \tag{11}$$

where the two leading terms $(1 + f_{21})(1 - f_{w2})$ represent the effect of wall-proximity, and f_{22} denotes the effect of free turbulence. The model functions f_{21} and f_{w2} are obtained by fitting the DNS data, which satisfy the limiting behavior of the wall:

$$f_{21} = \exp(-2 \times 10^{-4} R^{13})[1 - \exp(-2.2R^{0.5})] \tag{12}$$

$$f_{w2} = \exp(-5.5 \times 10^{-2} R_y - 5.0 \times 10^{-5} R_y^3 - 7.0 \times 10^{-9} R_y^5) \tag{13}$$

In Equation 12, R is the shear parameter derived from the scaling argument (Park and Sung 1995), $R = (Sk f_{w2})/(\varepsilon R_t^{1/2})$. Here, S represents the magnitude of strain rate, $S = \sqrt{2S_{ij}S_{ij}}$. The effect of free turbulence is also taken into consideration in the function f_{22},

$$f_{22} = 1 - 0.3\exp[-(R_t/6.5)^2] \tag{14}$$

which is obtained by curve-fitting the experimental results of grid-turbulence (Park and Sung 1995).

In the standard k-ε model, the production term P_ε^3 is generally neglected. However, the DNS data near the wall reveal that P_ε^3 is comparable to the turbulent diffusion term in the ε-budget. Therefore, it is necessary to balance the exact near-wall behavior of k and ε. Rodi and Mansour (1993) derived the following model terms by manipulating the Navier–Stokes equations

$$P_\varepsilon^3 = C_1 \upsilon \upsilon_t U_{,jj}^2 + C_2 \upsilon \left(\frac{k}{\varepsilon} \right) k_{,j} U_{,j} U_{,jj} \tag{15}$$

where $C_1 = 1.0$, and $C_2 = 0.006$. On the basis of this model, a slightly modified model is introduced in the present study by utilizing the wall-reflection function f_{w1}. This approach ensures that P_ε^3 be located within the wall layer $(y^+ \le 30)$

$$P_\varepsilon^3 = \left[C_1 \upsilon \upsilon_t S_{,j}^{*2} + C_2 \upsilon \left(\frac{k}{\varepsilon} \right) k_{,j} S^* S_{,j}^* \right] f_{w1} \tag{16}$$

where S^* is a modified strain rate parameter, which has the form $S^* = C_r \sqrt{\upsilon \varepsilon}\,/(\upsilon + \upsilon_t)$ (Park and Sung 1995). The model constant C_r is set as $C_r = 2.75$.

The summarized form of the ε-equation, which is used in the present study, is expressed in the following:

$$U_j \frac{\partial \varepsilon}{\partial x_j} = \frac{\partial}{\partial x_j} \left[\left(\upsilon + f_t \frac{\upsilon_t}{\sigma_\varepsilon} \right) \frac{\partial \varepsilon}{\partial x_j} \right] + 1.45(0.98 + 0.02P_k/\varepsilon) P_k \frac{\varepsilon}{k} - 1.9 f_2 \frac{\varepsilon^2}{k} + \left[C_1 \upsilon \upsilon_t S_{,j}^{*2} + C_2 \upsilon \left(\frac{k}{\varepsilon} \right) k_{,j} S^* S_{,j}^* \right] f_{w1} \tag{17}$$

Application to attached boundary layer flows

Before proceeding further, it is important to ascertain the generality and accuracy of the present model to an attached boundary layer. Toward this end, we have applied the model to a fully developed channel flow for which turbulence quantities are available from the DNS data (Mansour et al. 1988). As stressed earlier, a new $f_{\mu 2}$ function was proposed to improve the characterstics of wall damping function f_μ near the wall. By utilizing the $f_{\mu 2}$ model, the profiles of f_μ are shown in Figure 2, together with the DNS data. The AKN model and the model of Launder and Sharma (1974) (hereafter referred to as LS model) are also included for comparison. The selected Reynolds numbers are $Re_\tau = 395$. As is evident, very close to the wall $(y^+ \le 50)$, the f_μ prediction by the present model is shown to be better than those by the AKN model and the LS model.

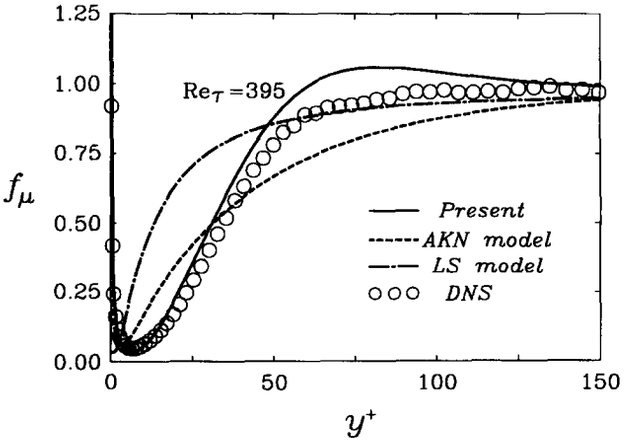

Figure 2 Comparison of the predicted f_μ with DNS (Re_τ = 395)

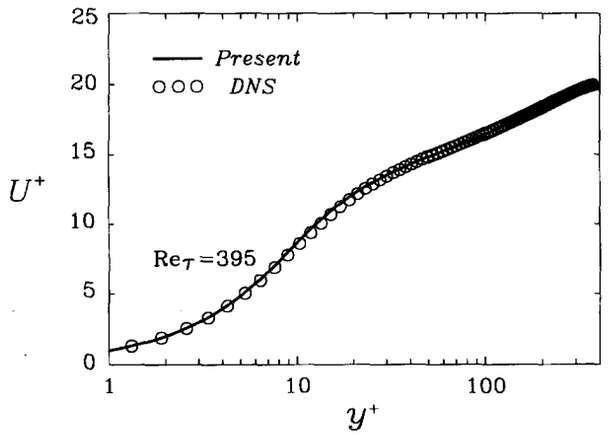

Figure 3 Comparison of the predicted U with DNS (Re_τ= 395)

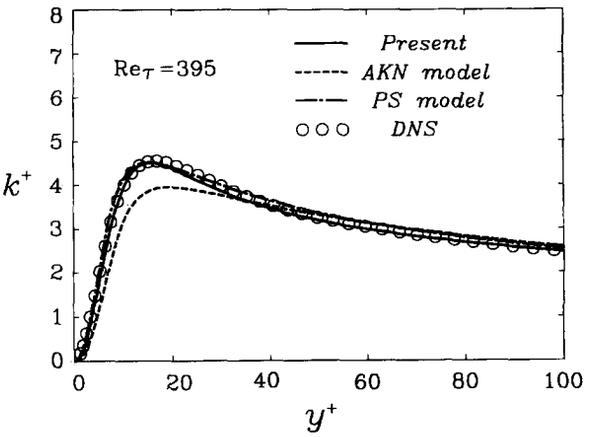

Figure 4 Comparison of the predicted k with DNS (Re_τ= 395)

The profiles of mean velocity, turbulent kinetic energy, and its dissipation rate are exhibited in Figures 3–5, respectively. The selected Reynolds number is $Re_\tau = 395$, for which DNS data exist. For the profile of mean velocity, the result of the present model is in good agreement with the DNS data in Figure 3. The profiles of turbulent kinetic energy k^+ are shown in Figure 4. The present model is seen to be in excellent agreement with the DNS data. The near-wall behavior of ε is displayed in Figure 5. In the ε^+ profiles, the result of the present model follows the DNS data fairly well. Furthermore, the maximum value of ε^+ very close to the wall is clearly displayed. It can be seen that the present model predictions are slightly improved as compared with those of Park and Sung (1995). The ε^+ profile of the AKN model overpredicts in the region $y^+ \leq 30$.

Accurate prediction of an adverse pressure gradient flow is crucial in simulating separated and reattaching flows. To assess the capability of the present model, the strong adverse pressure gradient flow is adopted for testing. The predicted result of C_f is shown in Figure 6, compared with the predictions of other models and the experiment of Samuel and Jourbert (1974). Obviously, the present prediction is in good agreement with the experimental data.

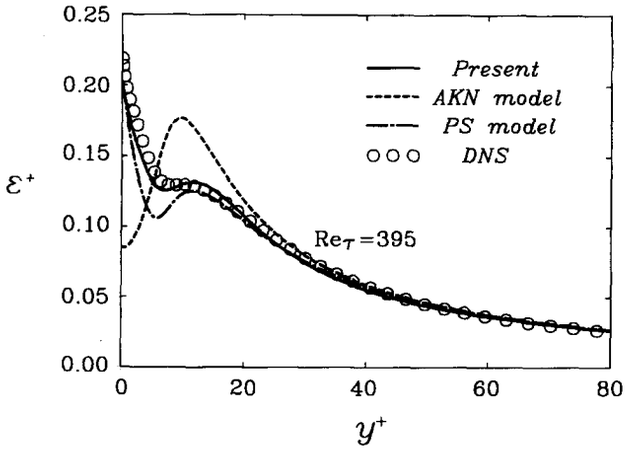

Figure 5 Comparison of the predicted ε with DNS (Re_τ= 395)

Application to the flows over a step with inclined wall

Numerical procedure

The finite-difference equations are discretized using the hybrid linear and parabolic approximation (HLPA) scheme with second-order accuracy. A nonstaggered variable arrangement is adopted with the momentum interpolation technique to avoid the pressure-velocity decoupling. The coupling between pressure and velocity is achieved by the SIMPLEC predictor-corrector algorithm, which is an improved version of the SIMPLE algorithm. The set of discretized linear algebraic equations is solved by a strongly implicit procedure (SIP) (Stone 1968).

The schematic diagram of flow configuration is shown in Figure 1. The inlet and outlet of the computational domain of the flows over a step with inclined walls are located $2H$ upstream and $30H$ downstream of the separation point, respectively. Here, H represents the step height. The inlet conditions are given from the experiment (Ruck and Makiola 1993). The no-slip boundary conditions are employed at the walls: $U = V = k = 0$, $\varepsilon_w = \upsilon \partial^2 k / \partial y^2$ and $\partial P / \partial y = 0$. The Neumann conditions are applied at the outlet.

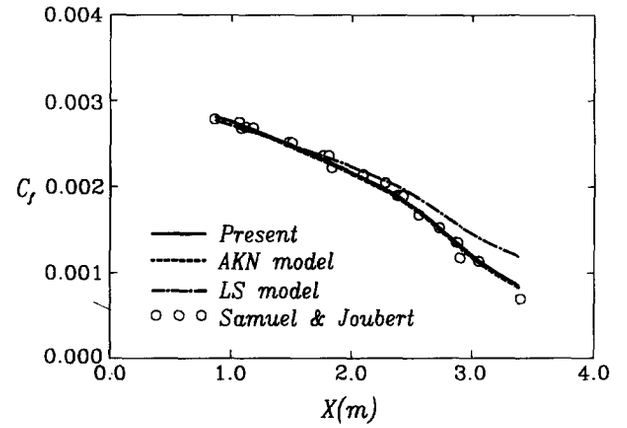

Figure 6 Comparison of predicted C_f with experiment in a strong adverse pressure gradient flow

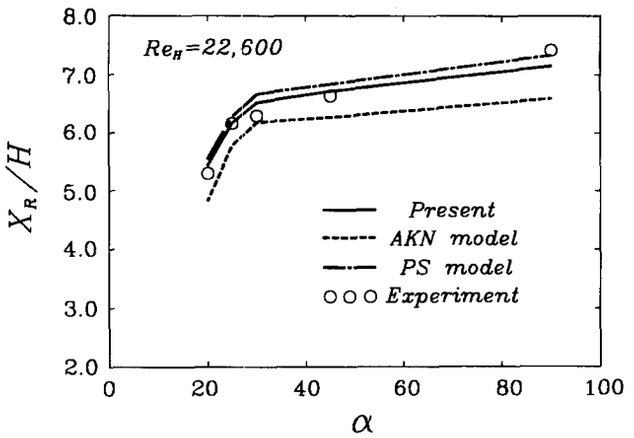

Figure 7 Comparison of the predicted X_R with experiment

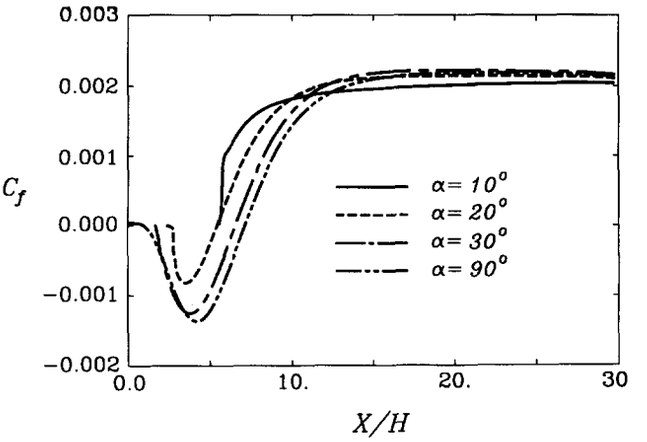

Figure 8 Skin friction coefficients

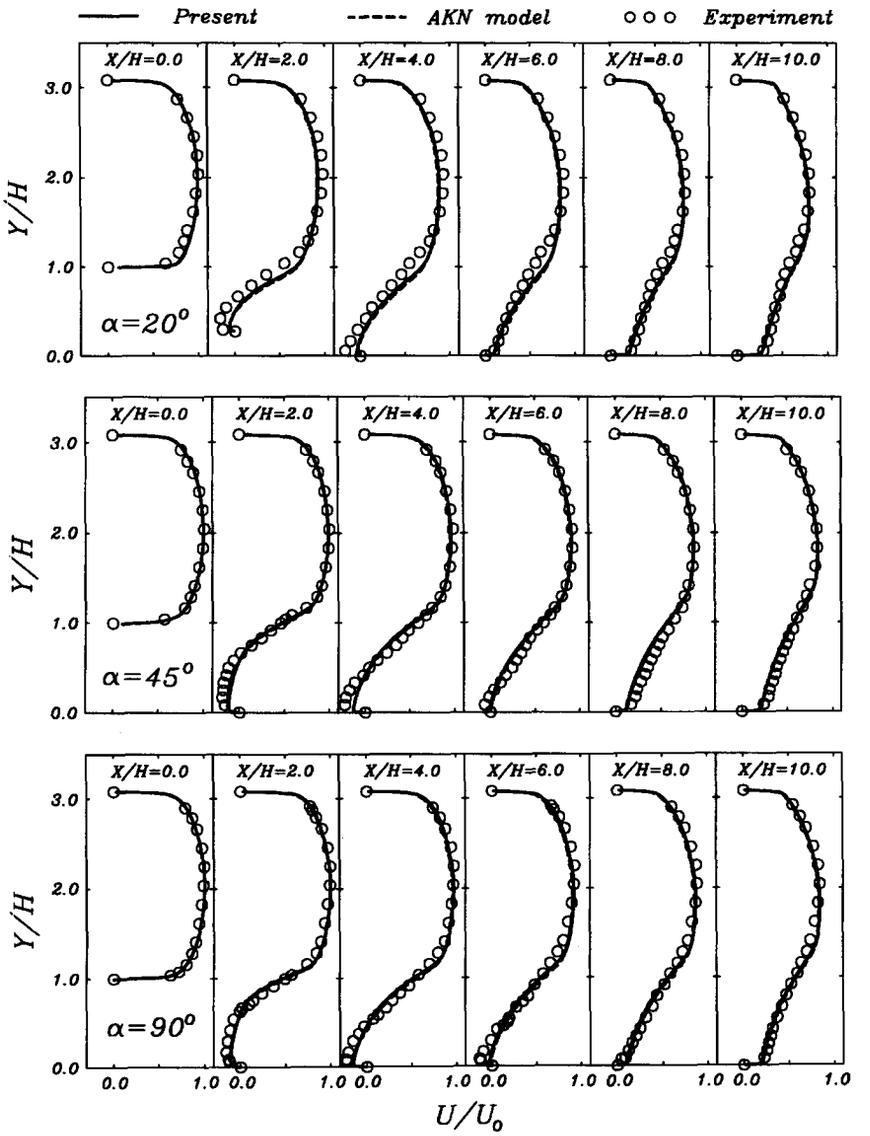

Figure 9 Comparison of the predicted U/U_0 with the experiment

The computations were implemented on a CRAY-YMP supercomputer, and a typical CPU time was approximately 3 hours for one set of calculations. Convergence was declared when the maximum normalized sum of absolute residual sources over all the computational nodes was less than 10^{-4}. The nonorthogonal grid systems were adopted for numerical calculations. The grid size was 200×100 for the flows ($\alpha < 90°$). For the flow over a backward-facing step ($\alpha = 90°$), the grid size was 200×120. The grid convergence was checked, and the outcome of these tests was found to be satisfactory.

Results and discussion

The main objective of the present study is to find a modified version of turbulence model, which can be applied with a reasonable accuracy to the flows over a step with inclined walls. Toward this end, the experimental data of Ruck and Makiola (1993) are employed to validate the present model performance. A schematic sketch of the flow configuration is shown in Figure 1, together with the coordinate (x, y) and the corresponding geometry. The graduations of inclined angle (α) are 10, 15, 20, 25, 30, 45, and 90°. The expansion ratio is $ER = 1.48$, and the Reynolds number based on the step height H is $Re_H = 22{,}600$.

Now, the reattachment lengths (X_R/H) at various inclined angles α are plotted in Figure 7. The computation results by employing the present model are represented together with the experimental data of Ruck and Makiola (1993). The results by the PS model and AKN model are also displayed. For the inclined angles of 10 and 15°, no separated and reattaching flows are exhibited in the computations as well as in the experiment. The calculated reattachment lengths by the present model agree reasonably well with the experiment for the most inclined angles. The reattachment lengths by the AKN model are underpredicted; whereas, those by the PS model are slightly overpredicted. As stated in the introduction, the PS model is shown to be the best performance at $\alpha = 90°$.

The skin friction coefficients (C_f) computed by the present model at various inclined angles α are plotted in Figure 8. For the inclined angle of 10°, only boundary-layer flow is presented

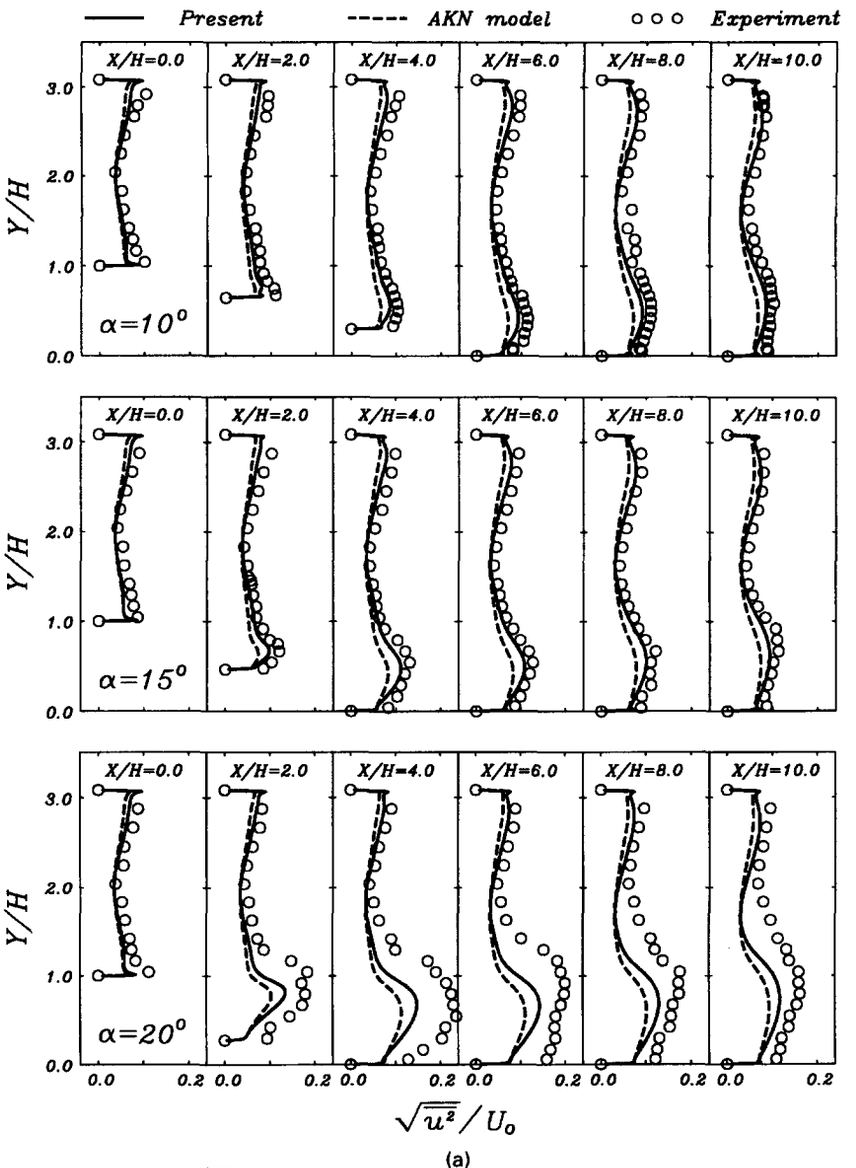

Figure 10 Comparison of the predicted $\sqrt{u^2}/U_0$ with the experiment

without negative skin friction. Because of this, the trend of skin friction coefficients at $\alpha = 10°$ is different from that of other inclined angles. For $\alpha \geq 20°$, the general features of the adverse pressure gradient flow are displayed. As α increases, the minimum value of C_f decreases. For $\alpha = 90°$, a small secondary recirculation zone is detected very close to the $X/H = 0$. The present computation results indicate that the flow field for $15° \leq \alpha \leq 20°$ is unstable, which may belong to the bifurcation region of flow separation.

Comparisons are extended to the distributions of the mean velocity profiles (U/U_0) and the streamwise velocity fluctuations $\sqrt{\overline{u^2}}/U_0$. The mean velocity profiles are plotted at six different stations in Figure 9. No noticeable differences are found in the mean velocity profiles predicted by the present model and AKN model for all angles. However, significant differences are displayed in the distributions of the streamwise velocity fluctuation $\sqrt{\overline{u^2}}/U_0$. The profiles of $\sqrt{\overline{u^2}}/U_0$ by employing the preceding two turbulence models are shown in Figure 10, in which the inclined angle is varied $10° \leq \alpha \leq 90°$. As can be seen in Figure 10, the predicted results of $\sqrt{\overline{u^2}}/U_0$ by the two models are generally underpredicted as compared with the experiment. However, the prediction by the present model is shown to be in close agreement with the experiment. The AKN model predictions are globally underpredicted. This discrepancy is thought to be the isotropic assumption of the AKN model, which is also addressed by Abe et al. (1994). Before separation; i.e., for $\alpha = 10, 15°$, the streamwise velocity fluctuations are seen to be mild. After separation, as α increases, the strengths of the streamwise velocity fluctuations also increase; i.e., the flow mixing in the recirculation region is augmented. It is interesting to find that the maximum value of $\sqrt{\overline{u^2}}/U_0$ at $\alpha = 20°$ is larger than that of $\alpha = 30°$. This means that, as mentioned earlier, the unstable flow separation is started around $\alpha = 20°$. Although the present model prediction is not entirely consistent with the experimental data, the present nonlinear model results are in better overall agreement than those given by the AKN model.

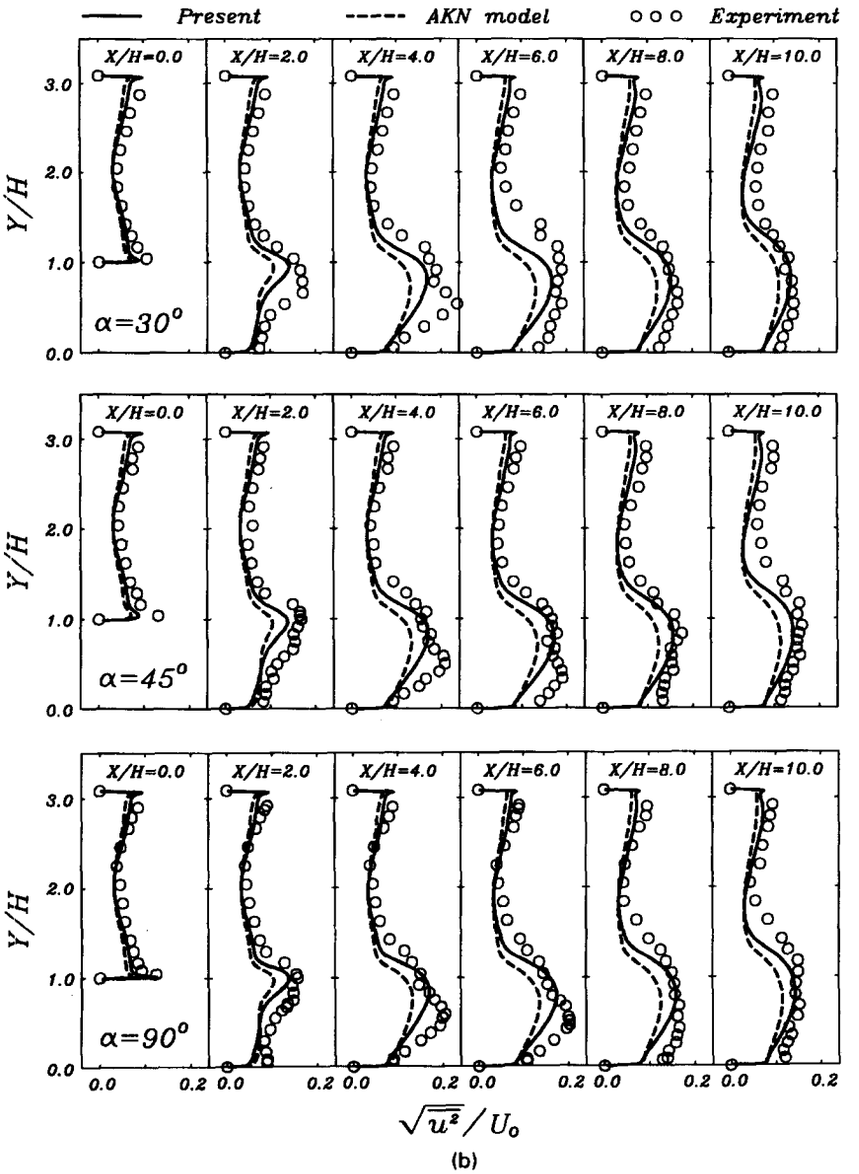

Figure 10 (continued)

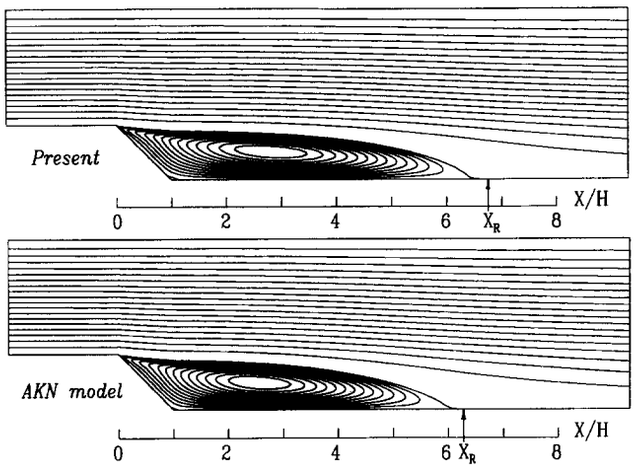

Figure 11 Comparison of the predicted streamlines ($\alpha = 45°$)

As shown earlier in Figure 7, the predicted reattachment lengths of the present model show good agreement with the experimental data; whereas, the AKN model underpredicts them. However, a closer inspection of the mean velocity profiles in Figure 9 reveals that both models show almost the same results for the mean velocity profiles. To make this issue clearer, comparisons of the predicted streamlines between the models are made in Figure 11 for $\alpha = 45°$. Although no big differences are detected in the mean velocity profiles, the predicted reattachment length of the present model ($X_R = 6.73$) is longer than that of the AKN model ($X_R = 6.25$).

To look into the flow evolutions in the recirculation region, the streamwise variations of the local maximum of the streamwise turbulent intensity $(\sqrt{\overline{u^2}_{\max}}/U_0)^2$ and the mean velocity $(U_{\max}/U_0)$ are displayed in Figures 12 and 13, respectively. The streamwise location is normalized by the reattachment length X_R

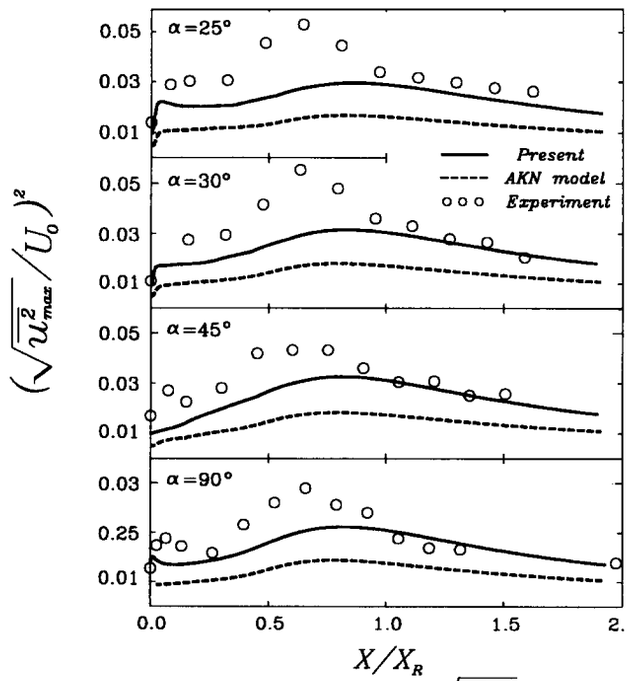

Figure 12 Comparison of the predicted $(\sqrt{\overline{u^2}_{\max}}/U_0)^2$ with the experiment

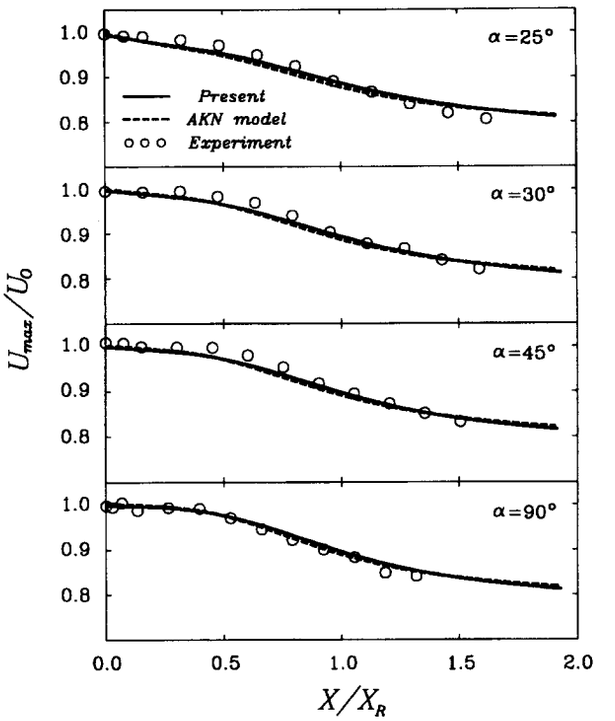

Figure 13 Comparison of the predicted decay law of $U_{\max}/U_0$ with the experiment

of individual step geometry. As shown in Figure 12, the model predictions by two models are also underpredicted compared with the experiment. Furthermore, the position of the peak value of $(\sqrt{\overline{u^2}_{\max}}/U_0)^2$ is not coincident. For example, the position of the experiment is $X/X_R \simeq 0.6$, while the position of the present computation is $X/X_R \simeq 0.8$. It is of interest to find that the position of the cross-sectional maximum turbulence intensity is little affected by the step angle inclination. However, the overall trend at each inclined angle is acceptable. The results by the AKN model are seen to be underpredicted significantly.

For the velocity decay in the streamwise portion of the velocity profile behind the step, the comparison between the experiment and the model predictions is shown in Figure 13. The results calculated by two models are seen to be in good agreement with the experiment.

Conclusions

The flows over a step with inclined wall, where a boundary-layer flow without separation and a separated and reattaching flow coexist, have been successfully simulated by employing the present model. To give a better prediction to the flows over a step with inclined walls, a slight modification of the PS model was made. A modified version of the $f_{\mu 2}$ function was employed to improve the characteristics of the wall-damping function f_μ near the wall. In the ε-equation, the nonequilibrium effect in recirculating region away from the wall was also incorporated. In the first, the present model was tested against the DNS data of a fully developed channel flow. It was shown that the present model predicts the f_μ distribution satisfactorily. Furthermore, the predicted results for k and ε reproduced the correct wall-limiting behaviors of the flow field. The computed results of the reattachment length by the present model were in good agreement with the experiment. While the reattachment lengths by the PS model were slightly overpredicted, those predicted by the

AKN model were underpredicted. The results of the mean velocity profile U by the present model followed well those of the experiment. Although no big differences were displayed in the mean velocity profiles, significant differences were shown in the streamwise velocity fluctuations ($\sqrt{\overline{u^2}}$). The computed results of $\sqrt{\overline{u^2}}$ by the present model were underpredicted slightly as compared with the experimental data. However, the results of $\sqrt{\overline{u^2}}$ by the present model were in better overall agreement in predicting the flows over a step with inclined walls than those by the AKN model.

References

Abe, K., Kondoh, T. and Nagano, Y. 1994. A new turbulence model for predicting fluid flow and heat transfer in separating and reattaching flows—1. Flow field calculations. *Int. J. Heat Mass Transfer*, **37,** 139–151

Avva, R. K. Kline, S. J. and Ferziger, J. H. 1988. Computation of the turbulent flow over a backward-facing step using the zonal modeling approach. Rep. TF-33, Stanford University, Stanford, CA, USA

Durbin, P. A. 1993. Application of a near-wall turbulence model to boundary layers and heat transfer. *Int. J. Heat Fluid Flow*, **14,** 316–323

Launder, B. E. and Sharma, B. I. 1974. Application of the energy dissipation model of turbulence to the calculation of flow near a spinning disc. *Lett. Heat Mass Transfer*, **1,** 131–138

Launder, B. E. 1982. A generalized algebraic stress transport hypothesis. *AIAA J.*, **20,** 435–437

Lee, M. J., Kim, J. and Moin, P. 1990. Structure of turbulence at high shear rate. *J. Fluid Mech.*, **216,** 561–583

Mansour, N. N., Kim, J. and Moin, P. 1988. Reynolds stress and dissipation rate budgets in a turbulent channel flow. *J. Fluid Mech.*, **194,** 15–44

Nagano, Y. and Shimada, M. 1993. Modeling the dissipation-rate equation for two-equation turbulence model. *Proc. 9th Symposium on Turbulent Shear Flows*, 23.2.1–23.2.6

Nagano, Y. and Tagawa, M. 1990. An improved k-ε model for boundary layer flows. *J. Fluids Eng.*, **112,** 33–39

Park, T. S. and Sung, H. J. 1995. A nonlinear low-Reynolds-number k-ε model for turbulent separated and reattaching flows. *Int. J. Heat Mass Transfer*, **38,** 2657–2666

Patel, V. C., Rodi, W. and Scheuerer, G. 1985. Turbulence models for near-wall and low Reynolds numbers flows: A review. *AIAA J.*, **23,** 1308–1319

Rodi, W. 1972. The prediction of free boundary layers by use of a two-equation model of turbulence. Ph.D thesis, University of London

Rodi, W. and Mansour, N. N. 1993. Low Reynolds number k-ε modeling with the aid of direct simulation data. *J. Fluid Mech.*, **250,** 509–529

Ruck, B. and Makiola, B. 1993. Flow separation over the step with inclined walls. In *Proc. Near-Wall Turbulent Flows*, Vol. 1, R. M. C., So, C. G. Speziale and B. E. Launder (eds.), 999–1008

Samuel, A. E. and Jourbert, P. N. 1974. A boundary layer developing in an increasingly adverse pressure gradient. *J. Fluid Mech.*, **66,** 481–505

So, R. M. C., Lai, Y. G. and Yoo, G. J. 1988. Low Reynolds number modelling of flows over a backward-facing step. *J. Appl. Math. Phys.*, **39,** 13–27

Stone, H. L. 1968. Iterative solution of implicit approximations of multidimensional partial differential equations. *SIAM J. Numer. Analysis*, **3,** 530–558

Yap, C. L. 1987. Turbulent heat and momentum transfer in recirculating and impinging flows. Ph.D. thesis, UMIST, Manchester, UK